

## 改进型溶胶-凝胶法制备粒径可调高染料吸附量 $\text{TiO}_2$ 微球及其在染敏电池光散射层中的应用

黄 欢<sup>1,2</sup> 魏玉龙<sup>1,2</sup> 包春雄<sup>1,2</sup> 高 皓<sup>1,2</sup> 于 涛<sup>\*,1,2</sup> 邹志刚<sup>1,3</sup>

(<sup>1</sup> 南京大学固体微结构物理国家重点实验室, 南京 210093)

(<sup>2</sup> 南京大学物理学院环境材料与再生能源研究中心, 南京 210093)

(<sup>3</sup> 南京大学材料科学与工程系, 南京 210093)

**摘要:** 利用改进型的溶胶-凝胶法, 制得了由锐钛矿相纳米颗粒组成的  $\text{TiO}_2$  多孔微纳小球。通过调节前驱物浓度, 合成出粒径可控的尺寸分别为 100, 175, 225, 475 nm 的  $\text{TiO}_2$  微纳小球, 并通过电泳沉积法将合成出的小球作为光散射层引入到染料敏化太阳能电池(DSSC)中。由于这种微纳小球在具备良好的光散射性能的同时也具备较高的染料吸附量, 因此相较于基于纳米颗粒的单层结构的 DSSC 拥有更高的光电转换效率。通过比较分析, 粒径尺寸为 475 nm 的微球作为光散射层的 DSSC 光电转换效率可以达到 6.3%, 较之于基于纳米颗粒的 DSSC 提高了 30%。

**关键词:** 粒径可控  $\text{TiO}_2$  微纳小球; 染料敏化太阳能电池; 散射层; 改进型溶胶-凝胶法

中图分类号: O614.41<sup>1</sup>; TM914.4

文献标识码: A

文章编号: 1001-4861(2013)10-2169-07

DOI: 10.3969/j.issn.1001-4861.2013.00.326

## Size-Controlled Nanoporous $\text{TiO}_2$ Spheres with High Dye-Loading: Facile Synthesis and Application as Scattering Layers in Dye-Sensitized Solar Cells

HUANG Huan<sup>1,2</sup> WEI Yu-Long<sup>1,2</sup> BAO Chun-Xiong<sup>1,2</sup> GAO Hao<sup>1,2</sup> YU Tao<sup>\*,1,2</sup> ZOU Zhi-Gang<sup>1,3</sup>

(<sup>1</sup> National Laboratory of Solid State Microstructures, Nanjing University, Nanjing 210093, China)

(<sup>2</sup> Eco-materials and Renewable Energy Research Center, Department of Physics, Nanjing University, Nanjing 210093, China)

(<sup>3</sup> Department of Materials Science and Engineering, Nanjing University, Nanjing 210093, China)

**Abstract:** Anatase nanoporous  $\text{TiO}_2$  spheres were synthesized via a modified sol-gel method. By controlling the concentration of the precursor, size-controlled nanoporous  $\text{TiO}_2$  spheres with high dye-loading were achieved. The synthesized spheres with different sizes (100 nm, 175 nm, 225 nm, 475 nm) were used as scattering layers on a  $\text{TiO}_2$  nanoparticle film by electrophoresis deposition method to form bi-layered dye-sensitized solar cells (DSSCs). Scattering effect of the layers with different sized spheres was studied. It was proved that the 475nm-sized spheres showed optimum light scattering effect. Due to the scattering effect, an overall photoelectric conversion efficiency of 6.3% has been achieved, a 30% increase compared with the nanoparticle-based photoanode.

**Key words:** size-controlled nanoporous  $\text{TiO}_2$  spheres; scattering layer; dye-sensitized solar cells

With more fierce energy crisis, interests on sustainable and renewable energy is keeping growing nowadays, among which solar cells have risen a worldwide attention. In the past two decades, Dye-sensitized solar cell (DSSC) has been considered as a promising alternative to conventional p-n junction solar

收稿日期: 2013-04-09。收修改稿日期: 2013-06-09。

国家自然科学基金(No.11174129)、江苏省自然科学基金(No.BK2011056, BE2012089)、中央高校基本科研业务费专项资金(No.1116020406)资助项目。

\*通讯联系人。E-mail: yutao@nju.edu.cn; 会员登记号: S02P210167M。

cell due to its low-cost fabrication process and efficient solar energy conversion efficiency<sup>[1-3]</sup>. A typical DSSC has a sandwich like structure consisting of a dye-adsorbed photoelectrode and a Pt counter electrode filled with an iodide/triiodide redox electrolyte. In the structure, the photoanode plays a crucial role in determining the light harvest and charge transport properties<sup>[4-7]</sup>. By using nanoparticles with the size of 10~20 nm, photoelectrode of conventional TiO<sub>2</sub>-based DSSC obtains a large surface area and therefore increases the dye adsorption<sup>[8]</sup>. However, photoanode fabricated using such nanoparticle form of TiO<sub>2</sub> is transparent to visible light and weak in visible light scattering due to the small particle size<sup>[9-11]</sup>. Hence, large particles have been deposited on top of the nanocrystalline photoanode as a scattering layer<sup>[12-13]</sup>. Recently, over 10% increase in the light-to-electricity conversion efficiency has been achieved by using 100nm-sized TiO<sub>2</sub> particles<sup>[14]</sup>. Meanwhile, the introduction of large particles into the photoanode will limit the performance of DSSC due to insufficient surface area and correspondingly decrease dye adsorption. One way to solve this problem is to use nanoporous TiO<sub>2</sub> spheres to get good scattering performance as well as effective dye adsorption.

Synthesis of TiO<sub>2</sub> spheres with selective size and crystal phase is crucial to the performance of scattering layer<sup>[15]</sup>. The phase of anatase is preferred than rutile for DSSC because of its larger band gap<sup>[16]</sup>, while the monodispersed spherical TiO<sub>2</sub> with a minimum size variation (less than 10%) is also preferred. Several methods like hydrolysis method and templating method have been used to obtain TiO<sub>2</sub> spheres<sup>[4,17-18]</sup>. However, synthesis of size-controlled monodispersed TiO<sub>2</sub> spheres is hard because hydrolysis speed is too fast.

In the present work, size-controlled monodispersed TiO<sub>2</sub> spheres were achieved via controlled hydrolysis and condensation of appropriate precursors<sup>[19]</sup>. The synthetic nanoporous TiO<sub>2</sub> spheres of anatase phase with a diameter ranging from 100 nm to 475 nm were used as the scattering layers of DSSCs. By achieving the effect of scattering effect as well as the high amount of dye adsorption, DSSCs with scattering layers show

superior light-electricity properties. By using the 475 nm-sized spheres, a 6.3% overall energy conversion efficiency has been achieved, indicating a 30% increase compared to photoanode using only nanoparticle film (4.75%). The scattering layer was fabricated by electrophoresis deposition (EPD) method due to its good performance in forming uniform layers with controllable thickness<sup>[20-22]</sup>.

## 1 Experimental

### 1.1 Synthesis of TiO<sub>2</sub> nanoparticles and porous TiO<sub>2</sub> Spheres with different sizes

Preparation of TiO<sub>2</sub> nanoparticles: an amount of 6 g (0.1 mol) of acetic acid was added dropwise to 29.3g (0.1 mol) of titanium iso-propoxide under vigorous stirring for 15 min at room temperature. Then the precursor was poured into 200 mL water as quickly as possible with vigorous stirring. 40 min was required to achieve a complete hydrolysis reaction. By adding 2 mL 65% nitric acid, the mixture was heated from room temperature to 80 °C in the water bath within 30 min and peptized for 1 h. Then water was added to adjust the volume to 150 mL as well as to cool down the liquid mixture. After heating at 210 °C in the autoclave for 12 h, the mixture was washed with ethanol for three times and then dried at 80 °C for 12 h.

Preparation of nanoporous TiO<sub>2</sub> spheres: to prepare the spherical titanium glycolate precursors, 0.2 mL, 0.5 mL, 0.8 mL, 1.1 mL titanium (IV) isopropoxide (TIP, 98%, Acros Organics) were added, respectively, to 10 mL ethylene glycol (EG, 99.8%, Nanjing Chemical Reagent Ltd.). After stirring for 10 min, the samples were quickly poured into an acetone bath (200 mL) containing trace of water (0.5 mL) under strong stirring for 20 min to form spherical colloids. By centrifuging and washing with ethanol for three times, the samples were dried in the air for 12 h at 80 °C. The samples were harvested by annealing at 500 °C.

### 1.2 Fabrication of dye-sensitized solar cells

To prepare the photoanodes of DSSCs, the synthesized TiO<sub>2</sub> nanoparticles, ethyl cellulose, terpinol with a mass ratio of 1:1:2, respectively, were added into ethanol under vigorous stirring. The paste was made by

rotary evaporation for 2 h in a 30 °C water bath. Then, the prepared paste was coated on the bare fluorine-doped tin oxide (FTO) glass using the doctor blade method. After drying for 10 min, the prepared film was calcined at 500 °C for 30 min (ramp rate 10 °C·min<sup>-1</sup>).

The scattering layers with different sizes of  $\text{TiO}_2$  spheres were fabricated by EPD method. In the process of electrophoretic treatment, the as-prepared film and a piece of bare FTO glass with a distance of 10 mm were used as the anode and cathode. Then the samples were placed parallelly in the suspension consisting of 100 mL acetone, 10 mg iodine and 50 mg  $\text{TiO}_2$  spheres. The EPD voltage was set at 15 V and held for various time to get different thicknesses of the scattering layer. The bi-layer film was then sintered over the same heating profile as previously. The calcined  $\text{TiO}_2$  electrode was immersed in a  $3 \times 10^{-4}$  mol·L<sup>-1</sup> solution of N719 (Solaronix S.A, Aubonne, Switzerland) in ethanol at room temperature for 24 hours.

The counter electrode, a magnetron sputter platinum mirror, was then clipped onto the top of the  $\text{TiO}_2$  photoanode to form a sandwich-like open cell. The electrolyte was composed of 1.0 mol·L<sup>-1</sup> BMII(1-butyl-3-methylimidazolium iodide), 50 mmol·L<sup>-1</sup> LiI, 30 mmol·L<sup>-1</sup> I<sub>2</sub> and 0.5 mol·L<sup>-1</sup> *tert*-butylpyridine in a mixed solvent of acetonitrile and valeronitrile.

### 1.3 Characterizations

To examine the crystallinity of as-prepared particles, X-ray diffraction patterns were collected on a Rigaku Ultimal III X-ray diffractometer (Cu K $\alpha$ ,  $\lambda = 0.15418$  nm) in the range of 10°~80° at a scan rate of 1°·min<sup>-1</sup> (2 $\theta$ ).  $\text{TiO}_2$  spheres were observed through Field-emission scanning electron microscope (FE-SEM, FEI NANOSEM 230, 15 kV). The BET surface area was measured on a Tristar micromeritics surface area analyzer. The film thickness was measured on a Dektak 6M stylus profiler. The transmission spectra were measured by a Cary 50 probe UV-Visible spectrophotometer. The test for photoelectric performance was taken on a Keithley 236 source measurement unit under AM 1.5 illumination with an active area of 0.132 cm<sup>2</sup>. The illumination was cast by Oriol 92251A-1000 sunlight simulator calibrated by the

standard reference of a Newport 91150 silicon solar cell. The incident monochromatic photo to electron conversion efficiency (IPCE) were measured by a self-built computerized apparatus<sup>[23]</sup>.

## 2 Results and discussion

### 2.1 Characterization

#### 2.1.1 XRD analysis

Compared with rutile  $\text{TiO}_2$ , anatase  $\text{TiO}_2$  is demonstrated to be more suitable for DSSCs<sup>[24]</sup>. According to the XRD patterns shown in Fig.1, no diffraction peaks of rutile or brookite phases of  $\text{TiO}_2$  are found, the phases of synthesized  $\text{TiO}_2$  nanoparticles and spheres are both pure anatase phase. The crystallite size of the samples can be estimated by the full width at half-maximum (FWHM) of the (101) peak of the anatase phase, based on the Scherrer equation. As a result, the calculated crystallite sizes of  $\text{TiO}_2$  nanoparticles and spheres (NS475, NS225, NS175, NS100) are 11.2 nm and 12.9 nm, 13.5 nm, 13.2 nm, 14.5 nm.

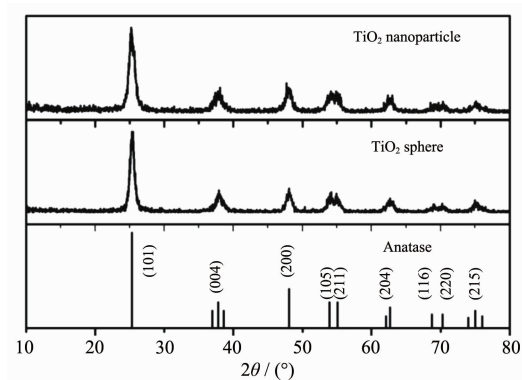


Fig.1 XRD of  $\text{TiO}_2$  powders for nanoparticle and sphere

#### 2.1.2 SEM analysis

Fig.2(a) and Fig.2(c) present the FE-SEM images of the as-synthesized nanoporous  $\text{TiO}_2$  spheres before and after annealing at 500 °C. Obviously, the spheres synthesized before annealing exhibit a well-defined spherical morphology with smooth surfaces. After annealing, the spherical nanoporous  $\text{TiO}_2$  are formed, turning the surface of the spheres to be rough. By changing the quantity of added TIP(0.2 mL, 0.5 mL, 0.8 mL, 1.1 mL), different sizes of nanoporous  $\text{TiO}_2$  spheres were achieved. As is shown in Fig.2 (c~f), the sphere sizes with a narrow distribution of less than 15% are

475 nm, 225 nm, 175 nm, 100 nm, respectively. From the results, we can see that the size of the  $\text{TiO}_2$  spheres can be controlled by controlling the concentration of titanium glycolate precursors in acetone. Research has found that an increase in water content in the hydrolysis reaction produces a higher nucleation rate<sup>[25-27]</sup> which leading to the formation of larger spheres. With the amount of TIP increasing from 0.2 mL to 1.1 mL, the water content in acetone decreases relatively, which makes the size of the achieved nanoporous  $\text{TiO}_2$  spheres decrease from 475 nm to 100 nm.

### 2.1.3 BET surface area analysis

The BET surface area of the  $\text{TiO}_2$  nanoparticles and spheres (NS475, NS225, NS175, NS100) are 118 and 98, 101, 103, 109  $\text{m}^2 \cdot \text{g}^{-1}$ , respectively. Fig.3 shows the  $\text{N}_2$  adsorption-desorption isotherm and pore size distribution of the 475 nm-sized  $\text{TiO}_2$  spheres. The type-IV isotherm with H2-type hysteresis loops at high relative pressures ( $P/P_0 = 0.65 \sim 0.95$ ) indicates a mesoporous structure<sup>[28]</sup>. According to the Barrett-Joyner-Halenda (BJH) model, the inset figure reveals a relative narrow pore size distribution in the range of

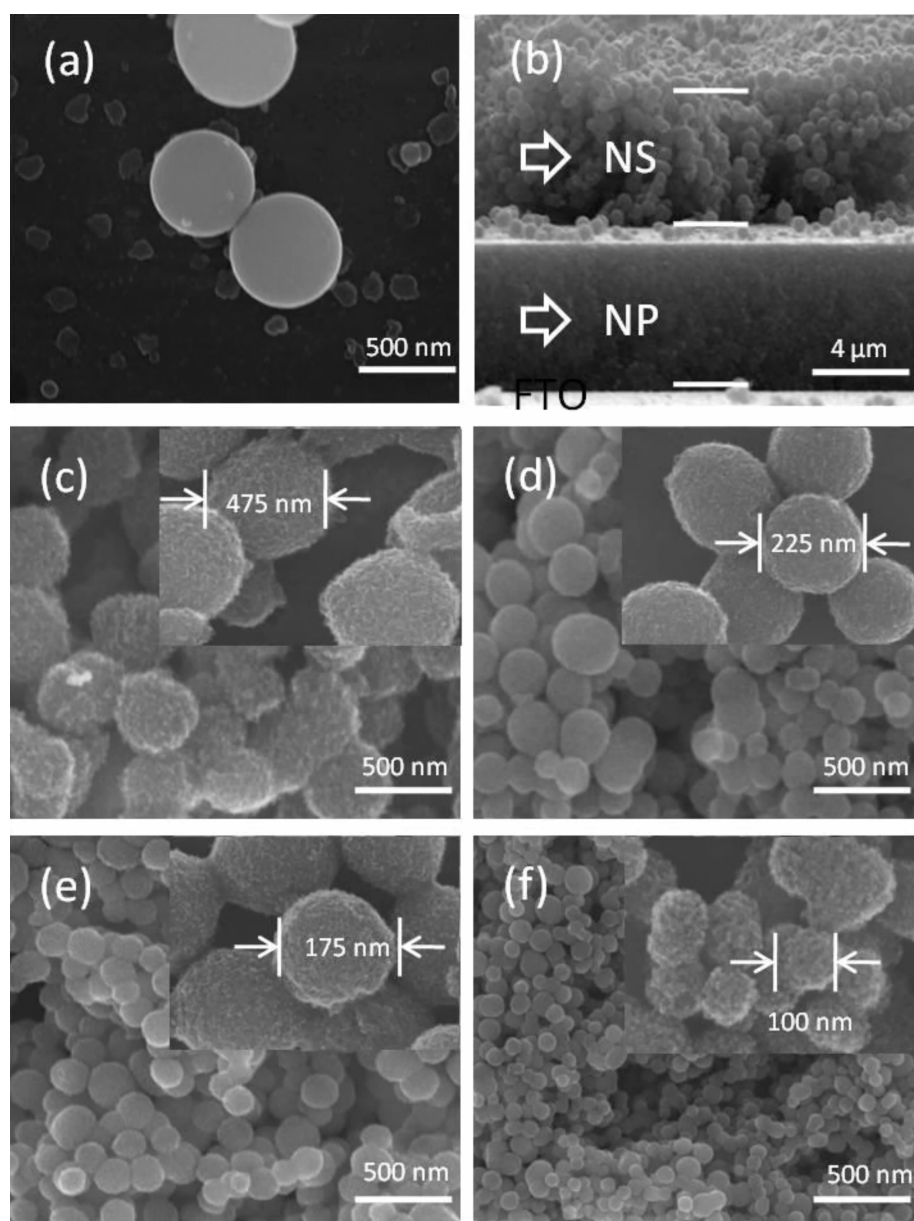


Fig.2 FE-SEM images of (a) as-synthesized spheres before annealing at 500 °C; (b) cross-section image of bi-layered DSSC; (c~f)  $\text{TiO}_2$  spheres with size of 475 nm, 225 nm, 175 nm, 100 nm

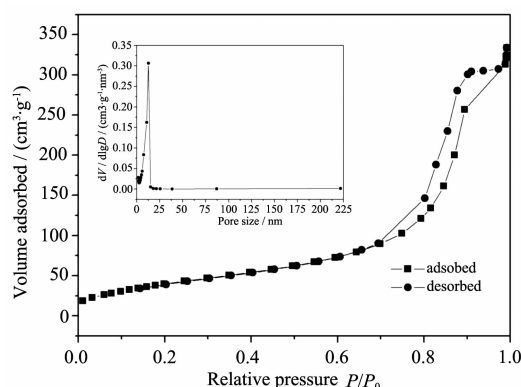


Fig.3 Nitrogen sorption isotherms and pore size distribution (inset) of the nanoporous  $\text{TiO}_2$  spheres (475 nm)

10 ~15 nm indicating that the  $\text{TiO}_2$  spheres are nanoporous.

## 2.2 Photovoltaic performance test

The as-synthesized nanoporous  $\text{TiO}_2$  spheres and nanoparticles were employed as photoanodes to assemble the DSSCs. A layer of nanoparticles (NP) was made using the doctor blade method while the scattering layers with different sizes of spheres (NS100, NS175, NS225, NS475) were made by the EPD method. Fig.2 (b) shows the cross-section FE-SEM image of the photoanode film. From the image, the thickness of the film is 12  $\mu\text{m}$ . The 475nm-sized spheres (NS475) were used as the scattering layer, the thickness of which is 6  $\mu\text{m}$ . For comparison, the thickness of a photoanode film assembled with NP was also controlled to 12  $\mu\text{m}$ . The current density-voltage ( $J$ - $V$ ) curves of DSSCs fabricated with two photoanode films (NP, NP+NS475) are shown in Fig.4. The corresponding photovoltaic parameters of the two cells are summarized in Table 1, including thickness of NP layer and NS layer, open circuit voltage ( $V_{\text{oc}}$ ), short circuit current density ( $J_{\text{sc}}$ ),

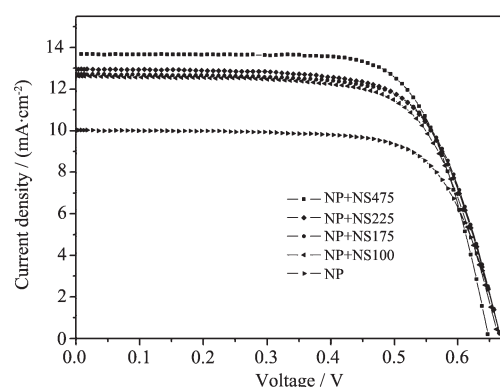


Fig.4  $I$ - $V$  curves of DSSC devices made with NS100, NS175, NS225, NS475 as the scattering layers

fill factor (FF), and efficiency ( $\eta$ ). We can see that the DSSC made of NP possesses an efficiency of about 4.75%. In contrast, the DSSC made of NP + NS475 shows a higher value of efficiency of about 6.3%, which represents a 32.6% enhancement compared to the former one.

Different sizes of  $\text{TiO}_2$  spheres (NS100, NS175, NS225, NS475) are employed as scattering layers in DSSCs (NP + NS100, NP + NS175, NP + NS225, NP + NS475) to study the scattering effect of  $\text{TiO}_2$  spheres. The thickness of the nanoparticle layer and scattering layer were adjusted to 12  $\mu\text{m}$  by controlling the time of electrophoresis deposition. Photovoltaic properties of the DSSCs are summarized in Fig.4 and Table 1. An obvious increase of  $J_{\text{sc}}$ , from 10.0  $\text{mA} \cdot \text{cm}^{-2}$  to 13.7  $\text{mA} \cdot \text{cm}^{-2}$ , is observed when the scattering layer is used. With the size of spheres increasing, more visible light is scattered so as to generate more photoelectrons, which has a positive effect on the photocurrent. The increasement in photocurrent also results in an improvement in photo-current conversion efficiency from 4.75% to 6.3%.

Table 1 Photovoltaic properties of the bi-layered DSSCs based on scattering layers with different sizes of spheres

Samples	NP Flim thickness / $\mu\text{m}$	NS Flim thickness / $\mu\text{m}$	Dye-loading / $(\text{mol} \cdot \text{m}^{-2})$	VOC / V	JSC / $(\text{mA} \cdot \text{cm}^{-2})$	FF / %	$\eta$ / %
NP	12.0 $\pm$ 0.1	0	4.71 $\times 10^{-7}$	0.668	10.0	70.9	4.75
NP+NS100	6.0 $\pm$ 0.1	6.0 $\pm$ 0.1	4.60 $\times 10^{-7}$	0.664	12.6	70.6	5.74
NP+NS175	6.0 $\pm$ 0.1	6.0 $\pm$ 0.2	4.52 $\times 10^{-7}$	0.667	12.7	70.0	5.93
NP+NS225	6.0 $\pm$ 0.1	6.0 $\pm$ 0.3	4.47 $\times 10^{-7}$	0.667	12.9	70.2	5.92
NP+NS475	6.0 $\pm$ 0.1	6.0 $\pm$ 0.5	4.35 $\times 10^{-7}$	0.650	13.7	71.0	6.30

To further study the scattering effect of the spheres, transmission spectra of the samples are characterized and shown in Fig.5. From the spectra, it is clearly that, with the size of the spheres getting larger, the transmittance of the cell is getting lower, which means the larger-sized spheres have a stronger scattering effect, attributed to enhancement of light harvesting by Mie scattering effect<sup>[29-31]</sup>.

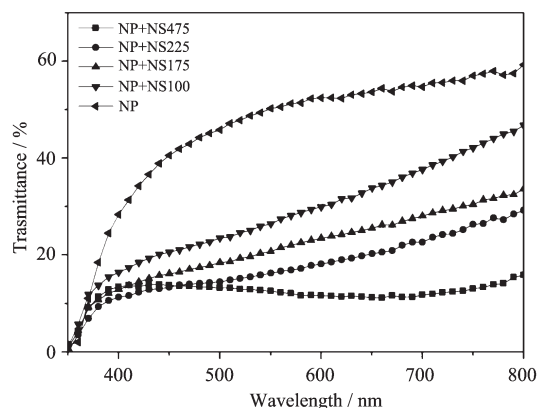


Fig.5 Transmission spectra of photoanodes using different sizes of  $\text{TiO}_2$  spheres as scattering layers

The incident-photo-current conversion efficiency (IPCE) spectra of the DSSCs is shown in Fig.6 to provide more evidence of the scattering effect. The DSSCs within scattering layers show a significant increase in IPCE over the wavelength range of 400~600 nm compared with the DSSC without scattering layers, implying that scattering layers enhance the photoelectric conversion efficiency of DSSCs. With the size of the spheres getting larger, the value of IPCE increases, which is in well agreement with the transmission spectra and circuit current density. Considering the amount of dye adsorption, the cells with scattering layers have almost the same dye-loading with the cell fabricated with nanoparticles, the amount of adsorbed dye per unit surface area (desorbed from the electrode by NaOH aqueous solution) are as follows: NP+NS100:  $4.60 \times 10^{-7} \text{ mol} \cdot \text{m}^{-2}$ , NP+NS175:  $4.52 \times 10^{-7} \text{ mol} \cdot \text{m}^{-2}$ , NP+NS225:  $4.47 \times 10^{-7} \text{ mol} \cdot \text{m}^{-2}$ , NP+NS475:  $4.35 \times 10^{-7} \text{ mol} \cdot \text{m}^{-2}$ , NP:  $4.71 \times 10^{-7} \text{ mol} \cdot \text{m}^{-2}$ . The relative high amounts of dye adsorption help the scattering layers scattering more light as well as absorbing enough dye to generate more photoelectrons

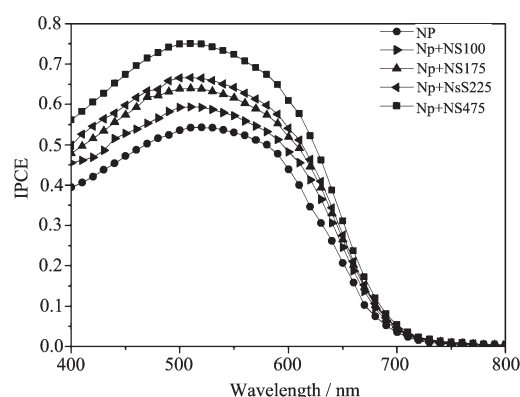


Fig.6 IPCE spectra of DSSCs: NP, NP+NS100, NP+NS175, NP+NS225, NP+NS475

than NP, which results in higher IPCE values in turn. The IPCE of the cell NP+NS475 reaches as high as 75% at the wavelength of 520nm indicating its better photoelectric performance, which is in well agreement with the I-V curve.

### 3 Conclusions

In present work, size-controlled anatase nanoporous  $\text{TiO}_2$  spheres with relative high dye-loading (100 nm, 175 nm, 225 nm, 475 nm) were synthesized via a modified sol-gel method by controlling the concentration of the precursor. The as-synthesized spheres with different sizes can be used as scattering layers on a nanoparticle  $\text{TiO}_2$  film by electrophoresis deposition method to form bi-layered dye-sensitized solar cells (DSSCs). Due to the effect of scattering effect as well as the high amount of dye adsorption, DSSCs with scattering layers show superior photoelectrical properties. It has been proved that the 475 nm-sized spheres have superior light scattering effect. Due to the scattering effect as well as the relative high dye-loading, an overall photoelectric conversion efficiency of 6.3% has been achieved, a 30% increase compared with the nanoparticle-based photoanode.

### References:

- [1] O'Regan B C, Grätzel M. *Nature*, **1991**,**353**:737-740
- [2] Grätzel M. *Nature*, **2001**,**414**:338-344
- [3] Grätzel M. *Inorg. Chem.*, **2005**,**44**:6841-6851
- [4] Wang H E, Zheng L X, Liu C P, et al. *J. Phys. Chem. C*,

- 2011,115**(21):10419-10425
- [5] Cheung K Y, Yip C T, Djuricic A B, et al. *Adv. Funct. Mater.*, **2007,17**:555-562
- [6] Wang Z S, Kawauchi H, Kashima T, et al. *Chem. Rev.*, **2004, 248**:1381-1389
- [7] Liu B, Boercker J E, Aydil E S, et al. *Nanotechnology*, **2008,19**:1-7
- [8] Tan B, Wu Y. *J. Phys. Chem. B*, **2006,110**:15932-15938
- [9] Yong W, Yu T, Liu B Q, et al. *Funct. Mater. Lett.*, **2012,5**:1-6
- [10] Hore S, Vetter C, Kern R, et al. *Sol. Energy Mater. Sol. Cells*, **2006,90**:1176-1188
- [11] Chen D, Huang F, Cheng Y B, et al. *Adv. Mater.*, **2009,21**: 2206-2210
- [12] Yang W G, Wan F R, Chen Q W, et al. *J. Mater. Chem*, **2010,20**:2870-2876
- [13] Huang F, Chen D, Zhang X L, et al. *Adv. Funct. Mater.*, **2010,20**:1-5
- [14] Wang Z S, Kawauchi H, Kashima T, et al. *Chem. Rev.* **2004,248**:1381-1389
- [15] Mou Pal, Garicia J, Santiago P, et al. *J. Phys. Chem. C*, **2007,111**:96-102
- [16] Kay A, Gratzel M. *Solar Energy Mater. Solar Cell*, **1996,44**: 99-117
- [17] Wang P, Zakeeruddin S M, Moser J E, et al. *J. Phys. Chem. B*, **2003,107**(48):13280-13285
- [18] Jung H G, Kang Y S, Sun Y K, et al. *Elect Acta*, **2010,55**: 4637-4641
- [19] Jiang X, Herricks T. *Adv. Mater.*, **2003,15**(14):1205-1209
- [20] Matthews D J, Kay A, Gratzel M. *Chem.*, **1994,47**:1869-1877
- [21] Grinis L J, Dor S, Ofir A, et al. *Photochem. Photobiol. A*, **2008,198**(1):52-59
- [22] TANG Ze-Kun(唐泽坤), HUANG Huan(黄欢), GUANG Jie (管杰), et al. *Chinese J. Inorg. Chem.(Wuji Huaxue Xuebao)*, **2012,28**:2401-2406
- [23] Xue G G. *J. Phys. D: Appl. Phys.*, **2013,45**:425104
- [24] Park N G, Van de Lagemaat J, Frank A J. *J. Phys. Chem. B*, **2000,104**:8989-8994
- [25] Nagpal V J, Riffe J S, Davis R M. *Colloids Surfaces*, **1994, 87**(1):25-31
- [26] Barringer E A, Bowen H K. *Langmuir*, **1985,1**(4):414-420
- [27] Parkar J C, Siegel R W. *Mater J. Res.*, **1990,5**(6):1246-1252
- [28] Park N G, Van de Lagemaat J, Frank A J, et al. *J. Phys. Chem. B*, **2000,104**:8989-8994
- [29] Ito S, Murakami T N, Comte P, et al. *Thin Solid Films*, **2008,516**(14):4613-4619
- [30] Qian J F, Liu P, Xiao Y, et al. *Adv. Mater.*, **2009,21** (36): 3663-3667
- [31] Frank A J, Kopidakis N, Coord J, et al. *Chem. Rev.*, **2004, 248**(13):1165-1179